Biophysical Chemistry 26 (1987) 63–70
Elsevier

BPC 01125

Protein structure probed by polarization spectroscopy

II. A time-resolved fluorescence study of human fibrinogen

A.U. Acuña [a], J. González-Rodríguez [a], M.P. Lillo [a] and K. Razi Naqvi [b]

[a] *Instituto de Química Física, C.S.I.C., Serrano 119, E-28006 Madrid, Spain*
and [b] *Department of Physics, University of Trondheim, N-7055 Dragvoll, Norway*

Received 26 November 1986
Accepted 16 December 1986

Fluorescence polarization; Rotational diffusion; Fibrinogen; Protein hydrodynamics

Human fibrinogen in solution was studied by monitoring the time-resolved depolarization of the fluorescence emitted by two spectroscopic labels of which the fluorescence lifetimes differ by an order of magnitude. Contrary to a long-held view, no evidence of molecular flexibility was found in the 10–1000 ns range. In addition, from the rate of the overall rotation, it is proposed that a prolate and symmetric ellipsoid of 47×10.5 nm may represent the time-averaged hydrodynamic size and shape of the protein in solution. This rigid and highly hydrated structure (4 g water/g protein) accommodates the latest nodular models obtained from electron microscopy, explains the singular hydrodynamics of fibrinogen and, apparently, it would perform the two main functions of the protein in haemostasis, blood coagulation and platelet aggregation, more efficiently than the flexible molecule.

1. Introduction

Proteins are known to exhibit, besides Brownian rotation and translation of the entire macromolecular framework, motions over an exceedingly wide time span, extending from about 10 ps to more than 1 s [1–3]. The universality and ubiquity of small-amplitude motions on the atomic scale have now been well documented [2,3], but instances of domain flexibility (i.e., motional freedom on a larger scale involving the concerted or cooperative movement of large segments of the macromolecule [4–6]) are less common; while motions of the former kind tend to preserve a unique time-averaged macromolecular conformation, the latter do not. The dynamic domains may coincide with the structural regions characterised by other biophysical or biochemical criteria; at any rate, their functional significance becomes easier to fathom out as the size of the flexible unit increases.

The plasma protein fibrinogen (M_r 340000) is usually described as a multidomain protein [7,8]. Electron-microscopic observations, conflicting at first, have now converged to a model very close to the elongated structure proposed by Hall and Slater [9], according to which the unhydrated molecule has overall dimensions of 45×4.7 nm and is made up of three nodular regions, named D, E, and D, co-linearly linked by three-stranded threads in a coiled-coil form [10]. A study of freeze-etched fibrinogen, conducted by Lederer and co-workers [11], indicated that the hydrated molecule is cylindrical, 45×9 nm in dimensions.

Correspondence address: A.U. Acuña, Instituto de Química Física, C.S.I.C., Serrano 119, E-28006 Madrid, Spain.

Abbreviations: FIB, human fibrinogen; 1,5-DNS, 1-dimethylaminonaphthalene-5-sulphonyl chloride; 1,5-DNS-FIB, 1,5-dansyl derivative of fibrinogen; MePy, methylpyrene; MePy-FIB, methylpyrene derivative of fibrinogen; GPIIb, glycoprotein IIb; GPIIIa, glycoprotein IIIa; D_t^0 and s^0, translational diffusion coefficient and sedimentation coefficient, respectively, at zero protein concentration.

According to early hydrodynamic measurements, reviewed by Doolittle [13], fibrinogen may be regarded as a prolate ellipsoid of revolution with an axial ratio (a/b) between 5 and 30, depending on the degree of hydration considered. Dynamic light scattering studies [14–16] suggested a rod-like structure 85–105 nm long and approx. 4 nm in diameter, which differs substantially from the cylindrical structures proposed by others [11,12]. In short, the size and shape of the fibrinogen molecule under physiological conditions are still in dispute.

The techniques of polarized fluorescence spectroscopy [17] provide useful information about the dynamic structure of proteins; measurements of the depolarization of fluorescence of suitable probes attached to the macromolecule, which can be carried out even under conditions close to physiological, are capable of revealing the size and shape and, if present, the flexibility of the proteins. The static non-isothermal version of the technique has already been applied to fibrinogen [18,19], and it has been concluded that this protein has considerable flexibility in the nanosecond time range; this conclusion is supported by the observation, in some electron micrographs [20], of bent and partially folded forms of fibrinogen. In the preceding paper [21], we presented new data on isothermal static polarization of labelled fibrinogen; these data negate the notion of a non-rigid fibrinogen and cast doubt on the hitherto accepted interpretation of the non-isothermal studies. In the work described here we pursue further the question of the domain flexibility in fibrinogen, by turning to time-resolved studies of fluorescence anisotropy. These dynamic measurements confirmed our picture of a rigid fibrinogen in the nanosecond time scale and the reinterpretation of the non-isothermal experiments presented before [21]. Furthermore, a model for fibrinogen in solution is elaborated by combining the rotational diffusion data, provided by the time-resolved experiments, with the experimental intrinsic viscosity. This model, an elongated and highly hydrated ellipsoid of revolution, explains the hydrodynamic properties of the molecule and accommodates the cylindrical objects photographed by the electron microscopists.

2. Experimental

2.1. Fibrinogen labelling

Human fibrinogen (Kabi, Stockholm) was purified as described before [21]. Two kinds of fluorescent derivatives of fibrinogen were prepared: 1,5-DNS-FIB, carrying the 1,5-dansyl chromophore, a short-lifetime label, and MePy-FIB, carrying the methylpyrene chromophore, a long-lifetime label. The detailed experimental procedures used in the preparation, purification, and biochemical and spectroscopic characterization of these derivatives have been described in the preceding paper [21]. The distribution of the label in both derivatives, determined by chemical and proteolytic fragmentation and subsequent analysis, was random over the surface of the protein molecule. The integrity and homogeneity of the samples used for spectroscopic measurements was checked before and after each experiment by electrophoresis, analytical high-performance size-exclusion chromatography, analytical ultracentrifugation and the measurement of the static fluorescence polarization.

Labelled fibrinogen samples used for spectroscopic experiments were dissolved (1 mg/ml) in 50 mM phosphate, 0.1 M NaCl, 1 mM EDTA, 0.025% NaN_3 pH 7.0. Samples used in experiments run at $T > 20\,^{\circ}C$ also contained aprotinin (0.1%). Blanks with unlabelled fibrinogen in the same buffer and at the same concentration were used to ascertain the abscence of fluorescent impurities and the light scattering contribution to the emission decay.

2.2. Time-resolved fluorescence anisotropy measurements

Time-resolved fluorescence data were collected in a time-correlated single-photon counting spectrometer. The excitation source consisted of a thyratron-triggered, N_2 flashlamp (Edinburgh Instruments EI 199), coupled to a 10 cm focal length monochromator. The fluorescence emission was isolated by a band-pass filter and detected by an RCA 8850 photomultiplier. The stop pulses were processed in a series of ORTEC NIM electronic

units and stored in an ORTEC multichannel analyser. Polaroid HNP'B plastic polarizers were used in the excitation and emission channels. The accumulated data were transferred to a PDP 11/05 minicomputer for analysis. Since the parallel and perpendicular intensity traces were accumulated sequentially, they must be scaled to correct for the fluctuations in the intensity and number of the excitation flashes. This was done by integrating the area under each curve [22] and comparing their ratio with that measured by stationary techniques under the same experimental conditions.

The fluorescence lifetimes were analyzed with a non-linear least-squares iterative reconvolution method [23–25]. This technique cannot be used in the analysis of the experimental decay of the fluorescence anisotropy $R(t)$, due to the limited capacity of the computer. Therefore, we used the method of moments [26,27], to deconvolve the experimental sum $S(t)$ and difference $D(t)$ functions (eq. 1).

$$R(t) = \frac{I_{\parallel}(t) - I_{\perp}(t)}{I_{\parallel}(t) + I_{\perp}(t)} = \frac{D(t)}{S(t)} \qquad (1)$$

The ratio of the deconvoluted functions was finally analysed using the non-linear least-squares method to obtain the correct rotational correlation times and amplitudes from the fitted anisotropy decay $r(t)$. The colour-shift of the stop photomultiplier (~ 2 ps/nm) was handled by the deconvolution routines as a linear time shift. The rotational correlation times presented here are the averaged values of at least 10 experiments, each with a different sample.

3. Results

3.1. 1,5-DNS-FIB, short emission lifetime derivative

The decay of the fluorescence of dansylated fibrinogen, 1,5-DNS-FIB, can be fitted to a two-exponential function, $i(t) = 0.6\ \exp(-9/t) + 0.4\ \exp(-20/t)$, although this is probably a simplified representation of a more complex decay, due to the variety of environments of the fluorescent label; the labelling ratio was about 5 dye molecules per fibrinogen molecule. The decay of the fluorescence anisotropy at 20 °C shows two distinct regions (fig. 1). In the short time range, a fast decay can be observed, with a time constant of 1 ± 0.5 ns, whereas in the remainder of the time window available for this particular fluorophore, the anisotropy shows a very slow decay with an apparent time constant larger than 600 ns. The fitting analysis did not include the first 7 ns of the experimental decay, where the contribution from the light scattered by the protein solution should be most severe, thereby losing some information on the most rapidly localized motion of the attached probe.

When the temperature of the protein solution is raised to 35.5 °C, the global picture of the anisotropy decay (fig. 1) is similar to that recorded at 20 °C. There is, however, an interesting difference: the contribution of the fast processes in the first 20 ns has clearly increased. The slowest fraction of the decay, on the other hand, is essentially parallel to that recorded at the lower temperature. In addition, there is no evidence of depolarizing motions in the 50–60 ns time range,

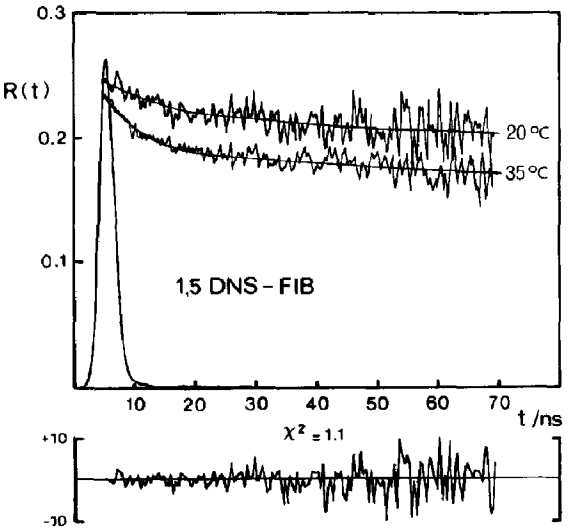

Fig. 1. Fluorescence anisotropy decay of 1,5-DNS-FIB (1 mg/ml) in phosphate buffer (pH 7.0), at two temperatures (excitation, 337 nm; emission, 450 nm long-pass cut-off filter). The smooth line is the fitted theoretical anisotropy function with two rotational correlation times: 1 ± 0.5 and 600 ± 50 ns.

which would be easily detected by this fluorophore. The slow time constant (> 600 ns) is so large, relative to the emission lifetime of 1,5-DNS-FIB, that it is interpreted here as a constant residual anisotropy convolved by a fitting artifact. The very low intensity of the polarized fluorescence, at times longer than two or three emission lifetimes, makes the analysis of the difference function $D(t)$ very uncertain under those conditions.

3.2. MePy-FIB, long emission lifetime derivative

This derivative was synthesized to explore the long times ranges that cannot be detected with the dansyl fluorophore. The MePy-FIB samples were dissolved in aerated buffer, and had a very low degree of labelling, approx. one fluorophore molecule per five fibrinogen molecules. However, as shown before [21], the MePy molecules are randomly bonded along the protein molecule, as in the case of the more heavily labelled 1,5-DNS derivatives. The decay of the emission of MePy-FIB is essentially single exponential between 60 and 500 ns, with a fluorescence lifetime of 105 ± 5 ns. At shorter times, a second emission component can be observed, with a lifetime of 15 ns, which accounts for less than 20% of the total fluorescence emission [23].

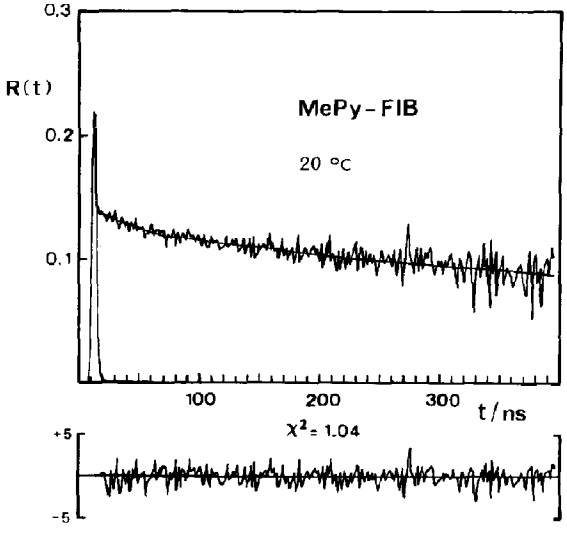

Fig. 2. Fluorescence anisotropy decay of MePy-FIB (1 mg/ml) in phosphate buffer (pH 7.0) at 20 °C (excitation, 337; emission, 450 nm long-pass cut-off filter). The smooth line results from the fitting of a theoretical anisotropy functions with two rotational correlation times: 6 ± 2 and 1100 ± 50 ns.

The time evolution of the fluorescence anisotropy of MePy-FIB (fig. 2) can be followed for almost 400 ns and, as in 1,5-DNS-FIB, the anisotropy decays by two different processes. In the first 60 ns a fast motion with a time constant of 3–8 ns was recorded, whereas the remaining fraction of the decay is very well described by a rotational correlation time of 1.1 + 0.15 μs. The error limits are mainly due to sample to sample variability, since this long correlation time is easily measured with reasonable accuracy.

4. Discussion

4.1. The rigidity of fibrinogen in solution

The results of the analysis of the anisotropy decay of 1,5-DNS-FIB (fig. 1) demonstrate that the only motions which depolarize the fluorescence of this derivative take place within the first nanosecond. Moreover, the $r(t)$ value at $t \to 0$ ($\simeq 0.25$) is considerably lower than the r_0 (0.312) determined at −20 °C in glycerol by static techniques [21], indicating the presence of unresolved subnanosecond motions of the fluorophore. These rapid motions, also detected in the isothermal stationary fluorescence depolarization study reported before [21,28], are assigned to the localized oscillation of the dansyl group in the protein. In fact, rotational correlation times in this time range have been measured directly [29] for this chromophore covalently bound to lysine, tyrosine, small peptides and enzymes. In addition, these fast motions of the label are the processes affected most by the 10 °C temperature increase (fig. 1). This effect might be analysed by introducing a temperature-dependent term in the angular motion of the label, although a qualitative approach would be enough for our purposes here. Since the relative weight of the subnanosecond components increased when the temperatures is raised from 25 to 35.5 °C this would produce a lowering in the

stationary anisotropy, if it is recorded in non-isothermal conditions. As a consequence, the time-resolved measurements give further support to the proposed [21] alternative interpretation of the steady-state depolarization data of Johnson and Mihalyi [18] and Hantgan [19]. Therefore, from both the steady-state and time-resolved results of 1,5-DNS-FIB it can be concluded that motions of large domains of the fibrinogen molecule in the 50 ns [18,19] time range are absent.

The analysis of the MePy-FIB anisotropy decay provides additional evidence on the intrinsic rigidity of fibrinogen in solution and extends up to 1000 ns the time range where motions of bulky segments of the molecule were not observed. The initial fraction of the decay and the large difference between $r(t)$ at $t \to 0$ ($\simeq 0.15$) and r_0, as measured by static techniques [21] at $-20\,^{\circ}$c in glycerol (0.217), can be explained by subnanosecond motions of the label, as above. On the other hand, the microsecond time constant is interpreted as being due to the overall tumbling of the protein and is discussed in detail below. Thus, human fibrinogen in solution appears as essentially rigid in the 10–1000 ns time interval.

4.2. Hydrodynamic size and shape

The experimental data on MePy-FIB from plots such as those of fig. 2 were fitted to the following expression:

$$r(t) = r_1(-t/\phi_L) + r_2(-t/\phi_P) \qquad (2)$$

where ϕ_L and ϕ_P represent the rotational correlation times of the label and protein, respectively. The value of ϕ_L (3–8 ns) depends on the exact location of the time origin in the fitting and reflects the fast motions of the fluorophore itself, while ϕ_P can be interpreted as arising from the rotational correlation time of the fibrinogen molecule. On the basis of this rotational correlation time, the absence of domain flexibility and the physico-chemical data accummulated in the past, we now attempt to gauge the hydrodynamical size and shape of the protein in solution.

We note first that a spherical shape, apparently supported by the experimental mono-exponential decay of $r(t)$, gives rise to marked contradictions in the predicted values of the coefficients of linear friction and viscosity. In addition, a sphere with a rotational correlation time of 1.1 μs would have a volume of 4500 nm^3 which, combined with the experimental value of the partial specific volume, 0.72 cm g^{-1} [13,30] would require a hydration of 7.2 g/g protein, which is an unreasonably high value.

We observe next that any elongated shape, approximated by a rigid prolate ellipsoid of revolution or by a cylinder with an axial ratio up to 8, will also show in our experiments a single-exponential decay of the fluorescence anisotropy; in spite of this the relevant theoretical expression of $r(t)$ [31] contains three exponential terms (eq. A1). This is just a consequence of two factors operating simultaneously: (i) the intrinsic averaging properties of the $r(t)$ expression for a symmetric ellipsoid randomly labelled and (ii) the short emission lifetime of the pyrenyl label relative to the fibrinogen rotational time. The effect of the first factor was examined by computer simulation of the anisotropy decay of model ellipsoids as a function of the axial ratio and volume [23] for a large variety of sizes. These computations showed that the decay of the fluorescence anisotropy deviates less than 10% from a single-exponential function in the first $3\phi_R$, even for very asymmetric rotors with axial ratios of 8 (ϕ_R, rotational correlation time of a sphere having the same volume as the ellipsoid). Therefore, elongated rotors cannot be excluded only on the basis of a single-exponential decay of the fluorescence anisotropy. Admitting this uncertainty, we compared the experimental rotational correlation time with the data on the intrinsic viscosity $[\eta]$ of fibrinogen, trying to determine the dimensions of the solid that would be consistent simultaneously with both hydrodynamic parameters. This procedure is conceptually identical to the use of the β function of Scheraga and Mandelkern [32], which has been applied frequently [13,30,33] to the fibrinogen molecule. By combining $[\eta]$ with the initial slope of the anisotropy decay ϕ_0 (see the appendix) and eliminating the volume V, a function similar to the δ function of Sheraga and Mandelkern [32] can be obtained, which is more sensitive to volume and shape changes [33] than the β function:

$$\frac{[\eta]M\eta}{\phi_0 kN_0T} = \frac{\nu}{6}\left(\frac{4}{F_\perp} + \frac{2}{F_\parallel}\right) \quad (3)$$

The left-hand side of eq. 3 is an experimental quantity whereas the right-hand side contains the Einstein-Simha factor [34,35] and the Perrin factors $F_\parallel$ and $F_\perp$ [36]. Since all these factors depend only on the axial ratio, the value of (a/b) can be derived by simple numerical operation, once the intrinsic viscosity and the initial slope of the anisotropy decay have been determined. With this value, the volume of the protein can be computed from eq. A6 (see the appendix).

There is a reasonable accordance in the literature on the $[\eta]$ for human fibrinogen, so we used an average value of 25 ± 1 cm^3 g^{-1} [12,13,30,33]. The value of $\phi_0 = 1.1 \pm 0.15$ μs was that measured here. According to this method, the hydrodynamic behaviour of fibrinogen in solution may be modelled by a rigid prolate ellipsoid of revolution (fig. 3), with an axial ratio of 4.5 ± 0.5, 47 ± 2 nm of major axis, 10.5 ± 0.5 nm of minor axis, and a volume of approx. 2700 nm^3. Spherical and oblate ellipsoidal shapes are unambiguously excluded. It is interesting to note that a particle of these dimensions, requiring approx. 4.2 g/g of hydration, reproduces the experimental translational diffusion and sedimentation coefficients of fibrinogen (table 1), in addition to the intrinsic viscosity and the fluorescence anisotropy decay time. The perpendicular rotational diffusion constant $D_\perp$ of this particle (table 1) also agrees with that determined recently from dynamic light scattering measurements [15].

Finally, one may use the semi-empirical equations for the rotational diffusion coefficients of rods developed recently [37] and, by computing the dimensions of the equivalent cylinder, estimate a cylindrical model. Accordingly, if the volume of the hydrated fibrinogen is kept close to 2700 nm^3, the protein might be modelled by a rod having essentially the same length as that of the ellipsoid, but with a diameter 20% shorter.

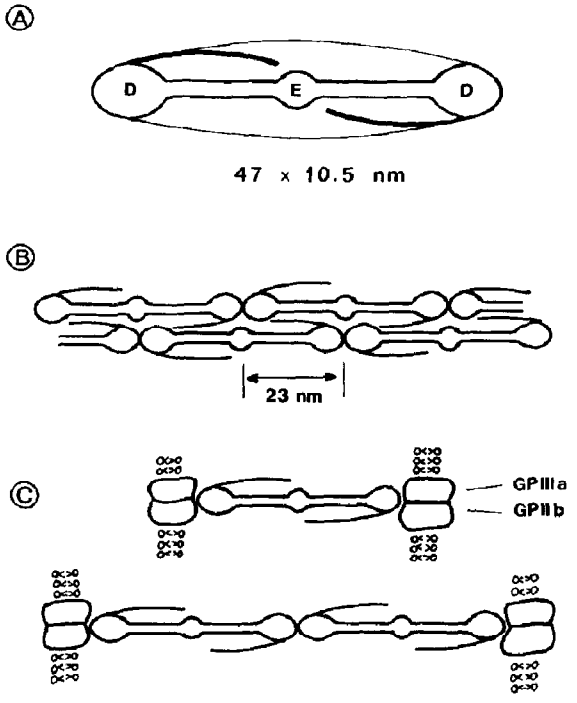

Fig. 3. Schematic diagrams of human fibrinogen and of its two main roles in a haemostasis. (A) Rigid ellipsoidal model proposed here, enclosing the string of beads observed by Hall and Slater [9]; (B) protofibril made of fibrin monomers after thrombin activation of rigid fibrinogen molecules; (C) cross-linking of platelets by fibrinogen during platelet aggregation.

4.3. Functional significance

The picture of fibrinogen in solution emerging from the work reported here is that of an elongated particle ($\sim 47 \times 10.5$ nm) with a stable conformation, i.e., essentially rigid (expression used with the same meaning as above), most probably with the C-terminal region of the γ chains ex-

Table 1

Comparison of the calculated hydrodynamic properties of a rigid prolate ellipsoid of dimensions 47×10.5 nm with the experimental values for human fibrinogen (in water at 20 °C)

Hydrodynamic property	Calculated	Experimental	Units	Reference
D_t^0	2.04	2.04 ± 0.08	10^7 cm^2 s^{-1}	30
s^0	7.98	7.79 ± 0.04	S	30
$[\eta]$	25	25 ± 1	cm^3 g^{-1}	11,30
D	6.2	5.0 ± 1.15	10^4 s^{-1}	15
ϕ_0	1.1	1.1 ± 0.15	10^{-6} s^{-1}	this work

tended to the centre of the molecule (fig. 3A), and carrying approx. 4 g water of hydration per g protein. This picture fits very well in what is currently known about the molecular mechanism of the two main functions of the haemostatic process in which fibrinogen is involved, viz., the formation of fibrin [38] and the aggregation of blood platelets [39]. As regards to the former, neither the mechanism of fibrin formation nor the 23 nm periodic structure of this fibre, i.e., half the length of a fibrinogen molecule, requires the existence of domain flexibility in the monomer; on the contrary, a rigid conformation of the fibrin monomer will presumably facilitate the non-covalent interactions responsible for the half-staggered array of fibrin molecules (fig. 3B) in the protofibril. As regards to the latter, it appears very likely that fibrinogen works as a bridge in platelet aggregation, cross-linking activated platelets [42], by interacting through its D domains with the unmasked fibrinogen receptors at the platelet surface, the glycoprotein complex GPIIb-GPIIIa [43,44]. If this is so, the rigid conformation of fibrinogen will avoid cross-linking two receptors at the surface of the same platelet by a single molecule, facilitating the interaction between receptors of two neighbouring platelets (fig. 3C).

Appendix

The decay of fluorescence anisotropy of a rigid ellipsoid bearing a randomly distributed fluorophore is expressed [31] by:

$$r(t) = r_0[0.4\exp(-t/\phi_1) + 0.4\exp(-t/\phi_2) + 0.2\exp(-t/\phi_3)] \quad \text{(A1)}$$

The rotational correlation times ϕ_L are functions of $D_\perp$ and $D_\parallel$, the perpendicular and parallel diffusion coefficients, respectively:

$$\phi_1 = (2D_\perp + 4D_\parallel)^{-1}; \quad \phi_2 = (5D_\perp + D_\parallel)^{-1}; \quad \phi_3 = (6D_\perp)^{-1} \quad \text{(A2)}$$

The initial slope of the $r(t)$ function can be easily obtained [40], and is given by:

$$\phi_0 = (4D_\perp + 2D_\parallel)^{-1} \quad \text{(A3)}$$

The diffusion constants can be conveniently replaced [41] by ratios of the frictional coefficients relative to the frictional coefficient of the sphere with the same volume (f_R). In this case, the equation for the initial slope becomes:

$$\phi_0 = \frac{6\eta V}{kT}\left(\frac{4}{F_\perp} + \frac{2}{F_\parallel}\right)^{-1} \quad \text{(A4)}$$

where each F is a rotational Perrin factor, which depends only on the ellipsoid axial ratio and is given by the ratio of the corresponding rotational frictional factors [41]:

$$F_\perp = f_\perp/f_R; \quad F_\parallel = f_\parallel/f_R \quad \text{(A5)}$$

Since the lifetime of the fluorophore in the time-resolved anisotropy decay of MePy-FIB is an order of magnitude shorter than the overall tumbling motion of the fibrinogen molecule, we concluded that the single-exponential decay of 1.1 μs, measured here, gives just the initial slope of the decay of $r(t)$, which extends for several microseconds. This assertion was confirmed by computer simulation of the $r(t)$ function of rotating cylindrical and ellipsoidal particles.

Finally, the intrinsic viscosity is given by [41]:

$$[\eta] = \nu N_0/M \quad \text{(A6)}$$

where ν is the Einstein-Simha factor, V the hydrated volume of the particle, M its molar mass, and N_0 Avogadro's constant. The values of ν as a function of the axial ratio were computed according to Simha [35].

Acknowledgements

We are grateful to Drs. F. Amat, J.J. Calvete and P. Usobiaga for their assistance in some of the physical and chemical analyses, and to Professor J. Garcia de la Torre for helpful discussions. This work was supported by Grant 1197/81 from the Comision Asesora de Investigacion Cientifica y Tecnica and by the Fondo de Investigaciones Sanitarias of Spain. K.R.N. thanks the University of Trondheim and the Norwegian Research Council for Science and Humanities (NAVF) for generous travel grants.

References

1 F.R.N. Gurd and T.H. Rothgeb, Adv. Protein Chem. 33 (1979) 73.
2 G. Carreri, P. Fasella and E. Gratton, C.R.C. Crit. Rev. Biochem. 3 (1975) 141.
3 M. Karplus and J.A. McCammon, C.R.C. Crit. Rev. Biochem. 9 (1981) 293.
4 J. Janin and S.J. Wodak, Prog. Biophys. Mol. Biol. 42 (1983) 21.
5 W. Bennet and R. Hubert, C.R.C. Crit. Rev. Biochem. 15 (1984) 291.
6 V.T. Oi, T.M. Vuong, R. Hardy, J. Reidler, J. Dangl, L.A. Herzenberg and L. Stryer, Nature 307 (1984) 136.
7 J.W. Weisel, C.V. Stauffacher, E. Bullitt and C. Cohen, Science 230 (1985) 1388.
8 R.F. Doolittle, Annu. Rev. Biochem. 53 (1984) 195.
9 C.E. Hall and H.S. Slater, J. Biophys. Biochem. Cytol. 5 (1959) 11.
10 F. Doolittle, D.H. Golbaum and R.F. Doolittle, J. Mol. Biol. 120 (1978) 311.
11 L. Bachmann, W.W. Schmitt-Fumian, R. Hammel and K. Lederer, Makromol. Chem. 176 (1975) 2603; K. Lederer, Makromol. Chem. 176 (1975) 2641.
12 M.C. Lopez Martinez, V. Rodes and J. Garcia de la Torre, Int. J. Biol. Macromol, 6 (1984) 261.
13 R.F. Doolittle, Adv. Protein Chem. 27 (1973) 1.
14 E.N. Serralach, V.E. Hofmann, M. Zulanf, T. Binkert, R. Hofman, W. Känzing, P.W. Straub and R. Schwyzer, Thromb. Haemostas. 41 (1979) 648.
15 P. Wiltzius and V. Hofmann, Thromb. Res. 19 (1980) 793.
16 M. Muller and W. Burchard, Int. J. Biol. Macromol. 3 (1981) 71.
17 J. Yguerabide and E.E. Yguerabide, in: Optical techniques in biological research, ed. D.L. Rousseau (Academic Press, New York, 1984) p. 275.
18 P. Johnson and E. Mihalyi, Biochim. Biophys. Acta 102 (1965) 476.
19 R.R. Hantgan, Biochemistry 21 (1982) 1821.
20 W. Fowller and H.J. Erickson, J. Mol. Biol. 134 (1979) 241.
21 A.U. Acuña, J. Gonzalez-Rodriguez, M.P. Lillo and K. Razi Naqvi, Biophys. Chem. 26 (1987) 55.
22 M.G. Badea and L. Brand, Methods Enzymol. 61 (1979) 378.
23 M.P. Lillo, Ph.D. Thesis, University of Madrid (1985).
24 A. Grinvald and I.Z. Steinberg, Anal. Biochem. 59 (1974) 583.
25 H.E. Zimmerman, D.P. Werthemann and K.S. Kaamm. J. Am. Chem. Soc. 96 (1974) 439.
26 I. Isenberg, R.D. Dyson and R. Hanson, Biophys. J. 13 (1973) 1090.
27 J. Yguerabide, Methods Enzymol. 26 (1972) 498.
28 A.U. Acuña and M.P. Lillo, International Symposium on Fluorescent Macromolecules, Bocca di Magra, Italy (1986).
29 G. Hoenes, M. Hauser and G. Pfleiderer, Photochem. Photobiol. 43 (1986) 133.
30 A.C.M. Van der Drift, A. Poppeman, F. Haverkate and W. Nieuwenhuizen, in: Fibrinogen: structure, functional aspects, metabolism, eds. F. Haverkate, A. Henschen, W. Nieuwenhuizen and P.W. Straub (Walter de Gruyter, Berlin, 1983) vol. 2, p.3.
31 M. Enhrenberg and R. Rigler, Chem. Phys. Lett. 14 (1972) 539.
32 H.A. Sheraga and L. Mandelkern, J. Am. Chem. Soc. 75 (1953) 179.
33 J.T. Yang, Adv. Protein Chem. 16 (1961) 323.
34 A. Einstein, Ann. Phys. (Lpz) 34 (1911) 591.
35 R.J. Simha, J. Phys. Chem. 44 (1940) 25.
36 F. Perrin, J. Phys. Rad. (Paris) VII-7 (1936) 1.
37 J. Garcia de la Torre and V.A. Bloomfield, Q. Rev. Biophys. 14 (1981) 81. (A factor of 1/4 is missing on the right-hand side of the expression for $D_{\|}$ in eq. 74.)
38 K. Bailey, F.R. Bettelheim, L. Lorand and W.R. Middlebrook, Nature 167 (1951) 233.
39 J.R. McLean, R.E. Mazwell and D. Hartley, Nature 202 (1964) 605.
40 P. Wahl, in: Time-resolved fluorescence spectroscopy in biochemistry and biology, NATO ASI Series A69, eds. R.B. Cundall and R.E. Dale (Plenum Press, New York, 1983) p. 497.
41 C.R. Cantor and P.R. Shimmel, Biophysical chemistry, part II (W.H. Freeman, San Francisco, 1980).
42 J.S. Bennet and G. Vilaire, J. Clin. Invest. 64 (1979) 1393.
43 R.L. Nachman, L.K. Leung, N. Kloezewiak and J. Hawiger, J. Biol. Chem. 259 (1984) 8584.
44 G.A. Marguerie, N. Thomas-Maison, M.H. Ginsberg and E.F. Plow, Eur. J. Biochem. 139 (1984) 5.